Mass and beta decay of ^{59}Mn†

R. C. Pardo,* C. N. Davids,‡ M. J. Murphy,§ E. B. Norman,§ and L. A. Parks‖
Physics Division, Argonne National Laboratory, Argonne, Illinois 60439
(Received 25 February 1977)

^{59}Mn was produced using the ^{48}Ca(^{13}C,pn)^{59}Mn reaction at $E_{^{13}C} = 26$ MeV. γ rays from the decay of ^{59}Mn were observed in singles and coincidence experiments using large Ge(Li) detectors after the targets were transferred to a shielded counting area by a multiple-target pneumatic transfer system. Assignment of γ rays to transitions in ^{59}Mn was confirmed by performing an ^{58}Fe($d,p\gamma$)^{59}Fe experiment. The half-life of ^{59}Mn was determined to be 4.6 ± 0.1 s. The results of this work limit the ground-state spin of ^{59}Mn to $5/2^-$ or $3/2^-$. Theoretical and systematic considerations favor $5/2^-$. The total β-decay energy, Q_β, was measured to be 5.2 ± 0.1 MeV, which corresponds to a mass excess of -55.5 ± 0.1 MeV.

[RADIOACTIVITY ^{59}Mn: measured $T_{1/2}$, E_γ, I_γ, γ-γ coin, E_β, β-γ coin; deduced decay scheme, logft limits, Q_β, g.s. J^π limit. Enriched targets, Ge(Li) detectors, plastic scintillator, multiple rabbit.]

INTRODUCTION

The β decay of the new isotope ^{59}Mn has been observed following its production via the ^{48}Ca(^{13}C,pn)-^{59}Mn reaction. The investigation of ^{59}Mn is part of a continuing program to study the decay properties of nuclei far from stability. These studies are useful for testing mass predictions and for establishing β-decay systematics, both of which are needed in nucleosynthesis calculations. ^{59}Mn is the third $T_z = \frac{9}{2}$ nuclide in the $1f$-$2p$ shell whose decay properties have been investigated in this program. A preliminary account of ^{59}Mn decay has appeared in Ref. 1. Studies of ^{51}Sc (Ref. 2) and ^{53}Ti (Ref. 3) decay have been previously reported.

The β-decay studies also provide a γ-decay scheme for states in the daughter nucleus. This information is useful in helping to understand the nuclear structure of the daughter.

The level structure of the ^{59}Mn daughter, ^{59}Fe, has been studied by Sperduto and Buechner,[4] Lee and Schiffer,[5] and Klema, Lee, and Schiffer[6] using the ^{58}Fe(d,p)^{59}Fe reaction. McLean *et al.*[7] were able to assign spins and parities to many of the levels observed in ^{59}Fe using the ^{57}Fe(t,p)^{59}Fe and ^{58}Fe-(d,p)^{59}Fe reactions.

Sood[8] attempted a Nilsson-model treatment of ^{59}Fe guided by the results obtained for ^{57}Fe in Ref. 9. McLean *et al.*[7] suggested that a different set of Nilsson-model parameters without bandmixing was needed to explain the levels observed in ^{59}Fe.

In the present paper we have measured the γ singles and γ-γ coincidence spectra following the β decay of ^{59}Mn. The assignment of γ rays to the decay of ^{59}Mn is based on the observation of the same γ rays in a concurrent ^{58}F($d,p\gamma$)^{59}Fe experiment. In addition, the energies of these transitions correspond to the deexcitation of levels previously observed in ^{59}Fe.

The total β-decay energy Q_β has been determined in a β-γ coincidence experiment. The resulting mass excess is compared with a recent measurement by Kashy *et al.*[10] and with various predictions.

The observed β-decay properties of ^{59}Mn allow restrictions to be placed on its ground-state spin and parity. A most probable spin is discussed in terms of theoretical expectations and systematics in this mass region. The observed γ-decay properties of levels in ^{59}Fe populated by the decay of ^{59}Mn are also discussed.

EXPERIMENTAL METHOD

A. Decay of ^{59}Mn: β^--delayed experiments

Initially, a beam of 50–100 nA (electrical) of 40-MeV $^{13}C^{4+}$ was allowed to bombard targets of enriched ^{48}Ca (96.8%) rolled foils 1.17 mg/cm^2 thick. Later runs were performed at a beam energy of 26 MeV. The calcium was placed on a 0.05-mm tantalum backing and a layer of gold, 100 μg/cm^2 thick, was flashed over the target to inhibit oxidation. During the initial survey experiments, a single target was sequentially bombarded in vacuum and pneumatically transferred to a remote counting station for observation by a Ge(Li) detector in close geometry perpendicular to the target. The apparatus used for this was a single-target pneumatic target-transfer system (rabbit). Control of bombardment, transfer of the target, and accumulation of data was accomplished by a quartz crystal sequence timer.

Data taken after this initial series of experiments employed a new multiple-target transfer device, "multiple rabbit," described in detail by Parks *et al.*[11] The multiple rabbit is an extension of the pneumatic target-transfer system mentioned above. After each bombard-transfer-count cycle, the used target is replaced by another target. The assembly is capable of holding up to eight different targets. After all targets have been used, the initial target is moved into place, and the entire cycle is repeated. All spectra shown and all results quoted in this paper are derived from experiments performed with this multiple rabbit system.

Data from γ-ray singles and γ-γ coincidence experiments were taken with "15% efficient" Ge(Li) spectrometers. These detectors viewed the target through 1.3-cm thick polyethylene absorbers. An NE102 plastic scintillator coupled to an RCA8575 phototube was used to detect β^- particles in coincidence with decay γ rays. Energy and efficiency calibrations for the detectors were performed using standard γ-ray sources.

γ-ray singles events were routed into six or eight 4096-channel time bins. Separate scaling of a pulser, gated by the busy signal from the analog-to-digital converter, provided dead-time information.

γ-γ coincidence data were event recorded on magnetic tape for subsequent off-line analysis. A coincidence resolving time of approximately 30 ns full width was used. Coincident γ-ray spectra of 2048 channels each were produced from events in one detector by setting windows in the other detector on γ-ray peaks of interest. These spectra were corrected for background-coincident events by subtracting spectra coincident with background regions just to the side of the γ ray of interest. The energy windows used were typically 3-4 keV full width.

B. γ transitions in ^{59}Fe

The only prior γ-ray study of transitions in ^{59}Fe was from the ^{58}Fe$(n,\gamma)^{59}$Fe work by Bogdanov *et al.*[12] Even with this work, the most recent compilation[13] quotes uncertainties in the energies of excited states of from 6 to 16 keV. Better energy assignments to these levels were necessary so that the interpretation of observed delayed transitions could be made with more confidence. The reaction ^{58}Fe$(d,p\gamma)^{59}$Fe was used to study the γ-ray transitions in ^{59}Fe. A 3.5-MeV deuteron beam of approximately 300 nA was provided by the Argonne National Laboratory Dynamitron accelerator. The target used was a 2.0-mg/cm^2 enriched (83.5%) ^{58}Fe foil. A natural Fe target was similarly bombarded in order to ensure that the γ rays observed were from reactions on ^{58}Fe. In-beam γ rays were detected at 90° with respect to the beam in close geometry using a 30-cm^3 Ge(Li) detector. The resolution of this detector was 9.0 keV at 1332 keV. This detector was chosen because it was felt to be sufficient for our needs and would be less sensitive to further damage by the high neutron flux encountered in this experiment.

RESULTS

A. Decay of ^{59}Mn: γ rays and half-life

In the survey runs using the single rabbit, five γ rays of energies 287.0, 472.7, 570.5, 591.0, and 726.1 keV were observed to decay with a half-life of 4-5 s. These γ rays appeared to correspond to the deexcitation of levels seen by McLean *et al.*[7] at energies of 287, 473, 574, 726, and 1162 keV. In addition, no nucleus was known to decay with γ rays of these energies and whose half-life was approximately 5 s.

The results of γ-ray energy measurements from the in-beam ^{58}Fe$(d,p\gamma)^{59}$Fe experiment are compared with the decaying γ rays initially observed in Table I. The 591-keV γ ray is not observed in the (d,p) experiment because it is obscured by the 596-keV transition from the ^{74}Ge$(n,n')^{74}$Ge reaction in the detector. The agreement between the in-beam γ-ray energies of the decaying γ rays is excellent. Therefore, the decaying γ rays observed are assigned to transitions in ^{59}Fe populated by the β decay of ^{59}Mn.

It was determined that the yield of ^{59}Mn relative to contaminant nuclei was maximized at 26 MeV and all subsequent data were accumulated at this bombarding energy. In order to measure the half-life of ^{59}Mn, singles γ-ray data were accumulated in eight time bins of 2 s each, after bombardment for 5 s. Figure 1 shows the data accumulated in the first two time bins summed together. The spectrum is displayed in square-root format so as to reduce the dynamic range.

The half-life of ^{59}Mn was determined using the composite decay curve for the γ rays of energies 287, 473, 571, 591, and 726 keV. The resulting half-life for ^{59}Mn is 4.6 ± 0.1 s.

TABLE I. Comparison of γ-ray energies observed in ^{58}Fe$(d,p\gamma)^{59}$Fe and delayed γ rays in ^{48}Ca + ^{13}C.

^{58}Fe$(d,p\gamma)^{59}$Fe (keV)	Delayed γ ray	Transition in ^{59}Fe
287.3 ± 1.0	287.0 ± 0.3	$287 \rightarrow 0$
472 ± 3	472.8 ± 0.3	$473 \rightarrow 0$
570.9 ± 1.0	570.7 ± 0.3	$571 \rightarrow 0$
727.1 ± 1.0	726.3 ± 0.3	$726 \rightarrow 0$
1210.6 ± 1.0		$1211 \rightarrow 0$

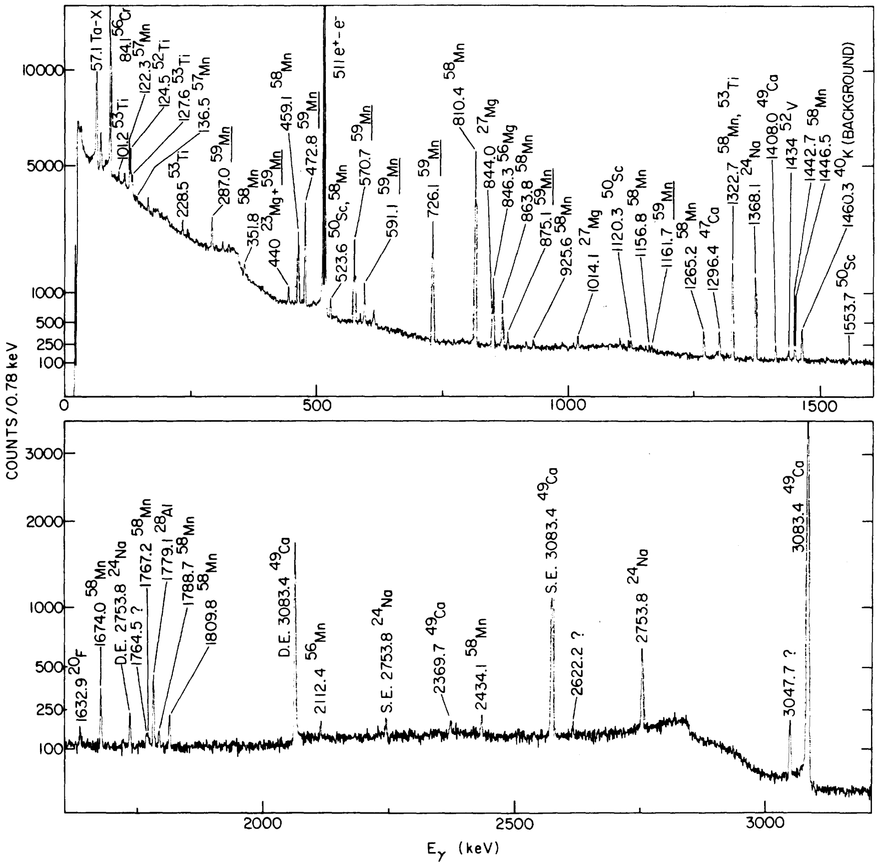

FIG. 1. Spectrum of delayed events during the first 4-s of count cycle from the $^{48}Ca+^{13}C$ reaction at 26 MeV. The data are shown in square-root format.

B. Decay of ^{59}Mn: Levels populated in ^{59}Fe and weak γ-ray transitions

In order to verify the assumed assignments of γ-ray transitions, and to search for weak transitions, a γ-γ coincidence experiment was performed. Spectra obtained in coincidence with three of the γ rays mentioned above are shown in Fig. 2. They have been corrected for background-coincident events. Two previously unassigned γ rays (439.6 and 874.7 keV) and, possibly a third (689 keV), were identified in the coincidence gates. The 689-keV transition, seen weakly in the 473-keV gate, yielded an intensity relative to the 726-keV γ ray ($I_{726}=100$) in the singles data of 0.6 ± 0.5. Also, setting a 473-keV gate in the second detector and looking at coincident events in the first yielded no coincident peaks. Therefore, this transition is considered only a possibility.

A careful search of the singles spectra revealed an additional decaying γ ray with an energy of 1162 keV which had a half-life consistent with that determined for ^{59}Mn. This γ ray was not observed in the coincidence experiments and is therefore assigned as a ground-state transition from the known 1162-keV level in ^{59}Fe.

A weak γ ray at 1021.9 keV was also observed in the summed spectrum of the first four time bins. This γ ray could be the ground-state transition from the population of the known level at 1026 keV. The random summing of two 511-keV γ rays would be expected to contribute 20–30% of the observed intensity but this mechanism does not seem to explain the entire peak. The intensity of the observed 1022-keV γ ray would yield an observed β-decay branch of 0.4 ± 0.3. This γ ray was not observed in coincidence in the β-γ experiments. Because there is no supporting evidence, the assignment of this γ ray to ^{59}Mn decay cannot be made.

The energies of the γ rays observed in ^{59}Mn and their relative intensities are summarized in Table II. The relative intensities quoted in Table II were obtained using the data of the first four time bins. Coincident summing corrections were applied where necessary. Because the 439-keV γ ray is a doublet in the singles γ-ray spectrum, its energy

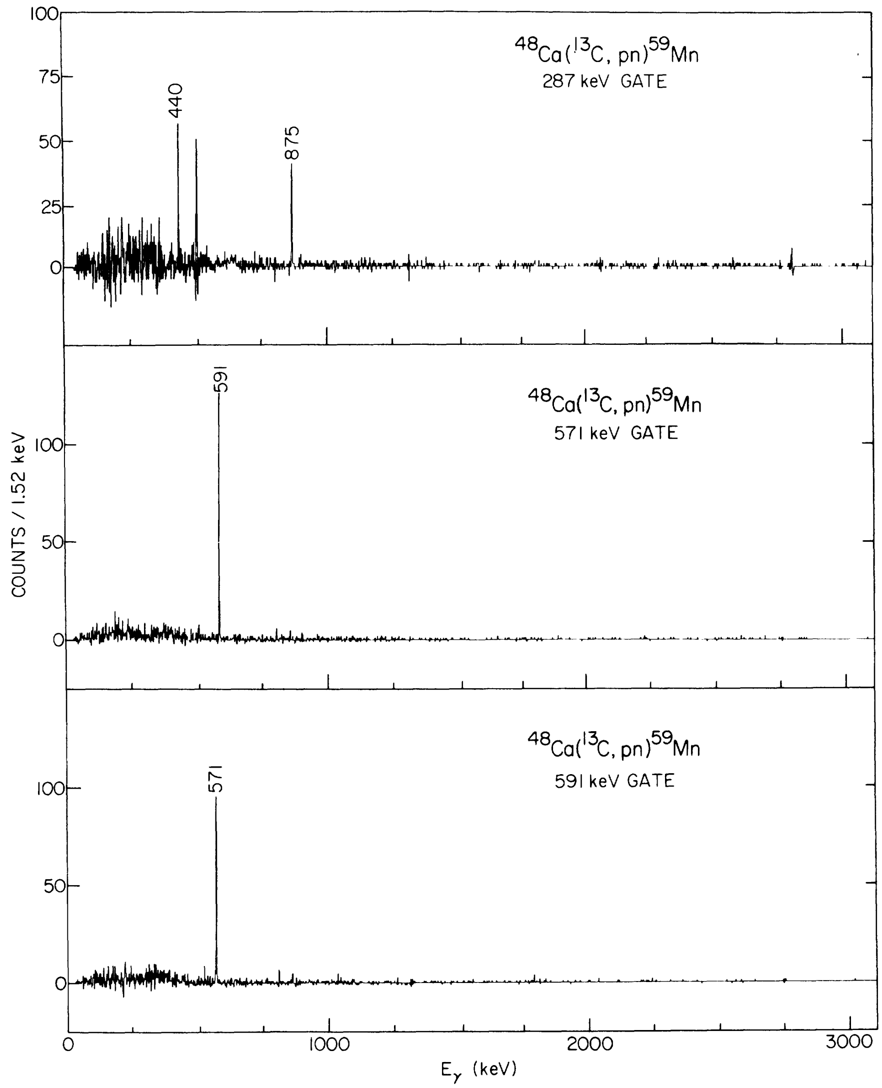

FIG. 2. γ-ray spectra observed in coincidence with the 287-, 571-, and 591-keV γ rays from the decay of ^{59}Mn. The unlabeled peak at 511 keV in the 287-keV gate is due to incomplete Compton background subtraction.

TABLE II. Energy and relative intensity of γ rays observed in the decay of ^{59}Mn.

Energy (keV)	Relative intensity
287.0 ± 0.3	12.9 ± 1.0
440 ± 1	4.5 ± 1.3
472.8 ± 0.3	69.1 ± 5.0
570.7 ± 0.3	58.8 ± 4.2
591.1 ± 0.3	22.5 ± 1.8
689 ± 2[a]	0.6 ± 0.5
726.3 ± 0.3	100
875.1 ± 0.7	6.7 ± 0.8
1161.7 ± 0.7	1.7 ± 0.7

[a]Possible transition, see text.

and relative intensity were obtained from the spectrum of events coincident with the 287-keV γ ray.

The resulting β-decay scheme for ^{59}Mn is shown in Fig. 3. The β feedings listed are taken directly from the observed γ-ray intensities and are calculated under the assumption of no ground-state branch. No corrections for internal conversion are made since the largest internal conversion coefficient is less than 0.003 if the observed transitions are $M1$. The $\log ft$ values listed assume no branch to the ground state and must be considered as lower limits. A Q_β value of 5200 keV has been used (see Sec. C below). The $\log f$ values are taken from the tables of Gove and Martin.[14]

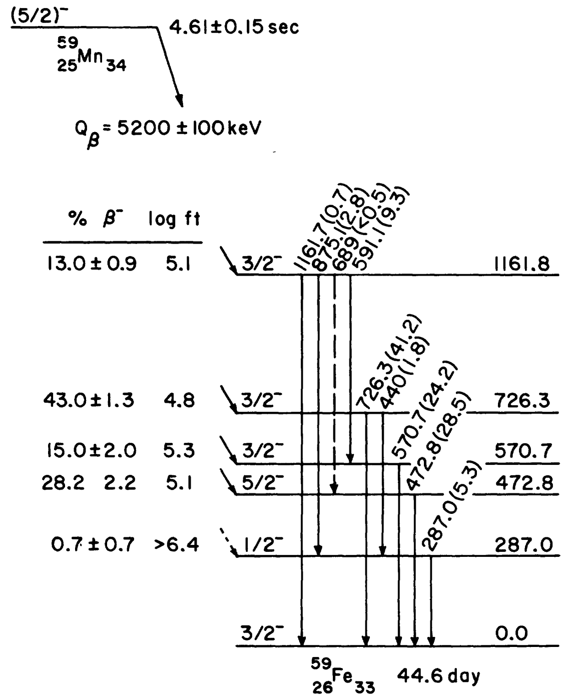

FIG. 3. The β-decay scheme of ^{59}Mn. Only those levels participating in the decay of ^{59}Mn are shown. The J^{π} assignments are taken from Ref. 7.

C. Mass of ^{59}Mn: β-γ coincidence

At about the same time this work was being performed, Kashy *et al.*[10] reported the observation of ^{59}Mn using the ^{64}Ni(^{3}He, ^{8}B)^{59}Mn reaction. This group found the mass excess of ^{59}Mn to be −55.49 ±0.03 MeV. Unfortunately, they were unable to resolve the ground state from a possible first-excited state in ^{59}Mn.

The total β-decay energy of ^{59}Mn has been measured using β-γ coincidence techniques. Data were cyclically accumulated for 10 s following a 5-s irradiation of the targets. The resulting γ-ray-gated β spectra for the strongest γ rays are shown in Fig. 4. These spectra have been corrected for background-coincident events.

The end-point energies of these β spectra were determined using the shape-fitting technique described by Davids *et al.*[15] This method employs a standard β-ray spectrum with a known end-point energy which is then stretched horizontally and normalized to reproduce the unknown spectrum. The standard used for this measurement was derived from the β spectrum coincident with the 3084-keV γ ray from the decay of ^{49}Ca. The isotope ^{49}Ca was produced simultaneously with ^{59}Mn by the reaction ^{48}Ca(^{13}C, ^{12}C)^{49}Ca. The resulting spectrum shown in Fig. 5 is a pure β^- spectrum with an end-point energy of 2184 ± 6 keV. The

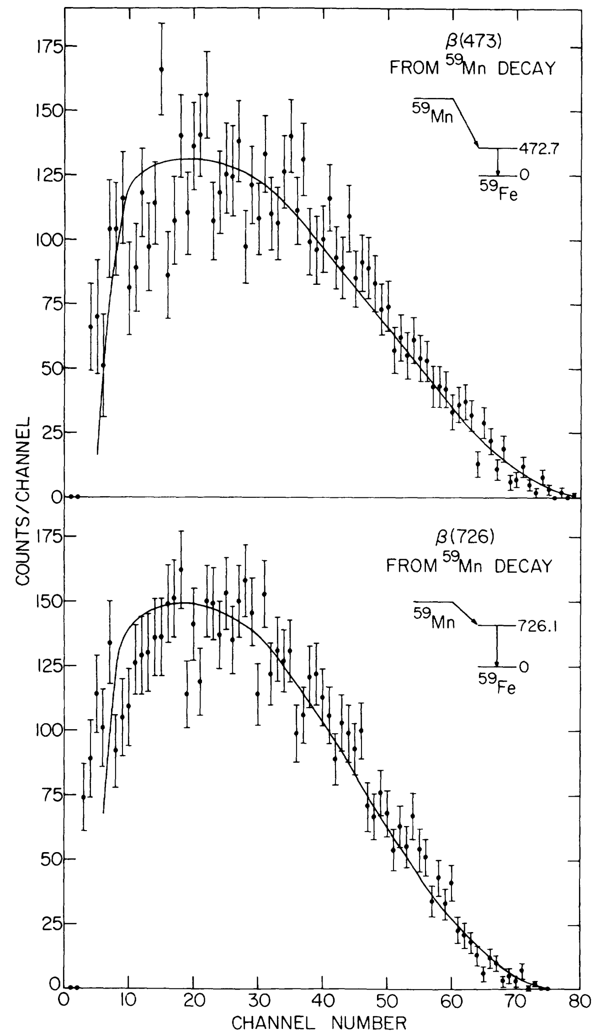

FIG. 4. Spectra of events coincident with selected γ rays in the decay of ^{59}Mn. These spectra were observed using an NE102 plastic scintillator. The smooth curve is a fit to the data by a stretch-fitting technique assuming the decay scheme shown in the inset.

smooth curve was drawn through the data by hand, and was then used as the standard shape. The accuracy of the hand fit was checked by shape-fitting the original ^{49}Ca data with this standard.

This method of analysis allows one to include the effects of coincident γ rays and multiple β feedings which may contribute to the resulting coincident spectra. The solid curves shown in Fig. 4 are the results of fits to the data assuming the decay schemes shown in the insets.

Similar γ-ray-coincident β spectra from other radioactive species with well-known β end-point energies were also produced. These spectra were shape-fitted using the techniques described above. The results are shown in Fig. 6. The straight line

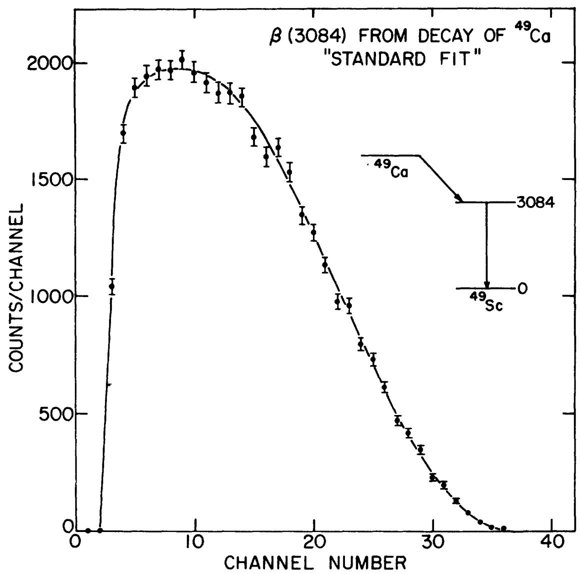

FIG. 5. Pure β spectrum coincident with the 3084-keV γ ray in the decay of ^{49}Ca. The smooth curve shown is hand drawn through the data. This curve is considered the "standard shape" of a single end-point β spectrum which is then used as described in the text to obtain the end-point energy of the β spectra from the decay of ^{59}Mn.

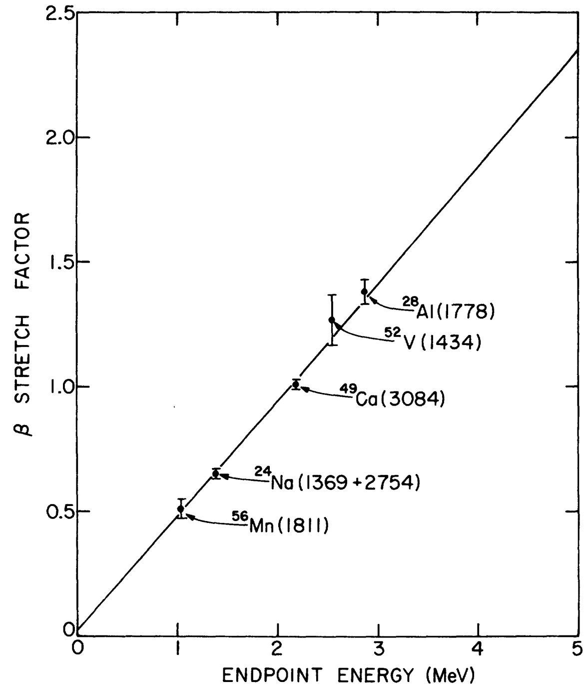

FIG. 6. The results of the stretch-fitting technique applied to the γ-ray coincident β spectra from nuclei with well-known β end-point energy, produced simultaneously with ^{59}Mn. The straight line is a linear least-squares fit to the data shown. This fit is used as the calibration for the determination of the end-point energies of β-decay branches in ^{59}Mn.

is a linear least-squares fit to the data. It is this fit to these internal calibrators which is used to obtain the β end-point energies of the transitions in ^{59}Mn. The values of the stretch parameter required to fit the various β spectra of ^{59}Mn are listed in Table III. This analysis yields a total β-decay energy Q_β of 5.2 ± 0.1 MeV. Using the value of the mass excess of ^{59}Fe from Wapstra and Bos,[16] the resulting mass excess of ^{59}Mn is -55.5 ± 0.1 MeV. This is in excellent agreement with the results of Kashy *et al.*[10] who obtain a value of -55.49 ± 0.03 MeV.

DISCUSSION

A. Ground-state spin of ^{59}Mn

The spins and parities of the states in ^{59}Fe observed in the decay of ^{59}Mn are known from the work by McLean *et al.*[7] From Fig. 3 it can be seen that the levels populated by β decay with a logft less than 5.3 have spins and parities of $\frac{3}{2}^-$ or $\frac{5}{2}^-$. The β-decay branch to the ground state of ^{59}Fe cannot be observed with our techniques. It is possible to estimate the intensity of this branch, in the context of the Nilsson model, using the observed feeding of the $\frac{5}{2}^-$ 473-keV state. If this state is the second member of the ground-state $K=\frac{3}{2}^-$ rotational band (see discussion below and Fig. 7), the β-decay branch to the ground state is related to the branch to the 473-keV state by the ratio of the squares of Clebsch-Gordan coefficients. A

TABLE III. Stretch-fit results for ^{59}Mn.

Nucleus	γ ray (keV)	Fit region channels	Stretch factor	χ^2_ν	Measured β^- end point (keV)	Q_β (keV)
^{59}Mn	473	5–71	2.24 ± 0.04	1.52	4676 ± 180	5273 ± 180
^{59}Mn	571	10–70	2.23 ± 0.06	1.07	4654 ± 203	5350 ± 203
^{59}Mn	591	17–59	1.86 ± 0.05	1.17	3858 ± 158	5145 ± 158
^{59}Mn	726	12–69	2.10 ± 0.02	1.40	4375 ± 149	5226 ± 149
					Average $Q_\beta = 5.2 \pm 0.1$ MeV	

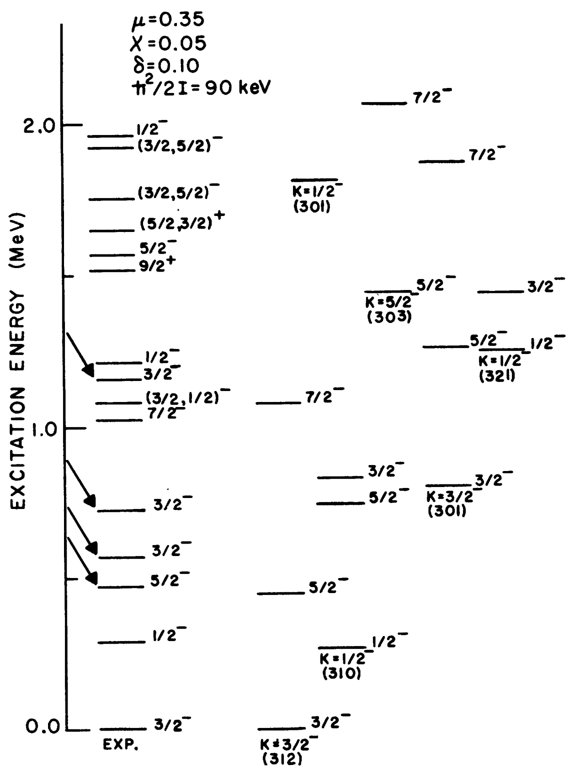

FIG. 7. Comparison of the known levels in ^{59}Fe to the predictions of a simple Nilsson model without bandmixing. The J^π assignments are from Ref. 7.

ground-state branch of 51% is thus predicted for the β decay of ^{59}Mn. The $\log ft$ values quoted would therefore be increased by approximately 0.3 from those listed in Fig. 3 if this branch is assumed. From the rules deduced by Raman and Gove,[17] these β transitions are definitely allowed. Therefore, in these β-decay branches J can change by 0 or ±1 with no change in parity. These observations restrict the spin of the ground state of ^{59}Mn to be either $\frac{3}{2}^-$ or $\frac{5}{2}^-$.

The $J^\pi=\frac{1}{2}^-$ level at 287 keV is fed from higher energy states by the 439- and 875-keV γ rays. The data from this work are consistent with no β feeding to this level, but a small feeding with a $\log ft > 6.4$ cannot be ruled out.

As discussed in the results section, the existence of a β-decay branch to the $J^\pi=\frac{7}{2}^-$, 1026-keV state in ^{59}Fe could not be confirmed. If this state is a member of the ground-state rotational band in ^{59}Fe, the same arguments as used above for the ground-state β-decay branch predict a total β-decay branch to the state of only 1.4%. This value is at or below the level of sensitivity achieved in this experiment. The observation of such a branch would have allowed a unique experimental determination of the ground-state spin of ^{59}Mn.

The simple shell model would predict the ground-state spin of all odd-A isotopes of manganese to be $\frac{7}{2}^-$. In fact, ^{53}Mn is the only manganese isotope known to have a ground-state spin of $\frac{7}{2}^-$. Both ^{55}Mn and ^{57}Mn have ground-state spins of $\frac{5}{2}^-$, as does ^{51}Mn. Ths isotopes ^{51}Mn, ^{55}Mn, and ^{57}Mn have $J^\pi=\frac{7}{2}^-$ first-excited states while ^{53}Mn has a $\frac{5}{2}^-$ first-excited state. The first-excited state of these odd-A manganese isotopes are all at less than 400 keV in excitation. The second-excited state of these isotopes is around 1 MeV and is often a $\frac{3}{2}^-$ state. From the systematics of these odd-A manganese isotopes, the assignment of $\frac{5}{2}^-$ for the ground state of ^{59}Mn would be favored.

As will be discussed more fully below, the structure of ^{59}Fe may be understood with the aid of the Nilsson model for deformed nuclei. Sood and Hutchinson[9] found the level structure of ^{57}Fe to be well reproduced using bandmixing in the Nilsson model. Both ^{57}Fe and ^{59}Fe are one neutron away from a ^{58}Fe core. Likewise, ^{59}Mn might be described by a single proton coupled to a ^{58}Fe deformed core. Specifically, the deformation parameter δ must take values in the range 0.1 to 0.14 to obtain agreement with the data. The positive nuclear quadrupole values in this region support a positive δ. The simple Nilsson model (without bandmixing) predicts the ground state of ^{59}Mn to be $\frac{5}{2}^-$. This prediction is independent of the exact value of δ so long as δ is positive. A $\frac{3}{2}^-$ ground state would be expected in this model only if δ were negative. Based on both the systematics of the manganese isotopes and the Nilsson model, the $\frac{5}{2}^-$ assignment for the ground state of ^{59}Mn is favored.

B. Levels in ^{59}Fe

Prior to the experimental work of McLean *et al.*,[7] Sood[8] attempted a theoretical description of the then known level structure of ^{59}Fe using the Nilsson-model description. Good agreement was obtained for the known levels using parameters in the Nilsson model which were not too different from the results Sood and Hutchinson[9] found necessary to describe the level structure of ^{57}Fe. Sood noted that bandmixing due to Coriolis coupling did not seem to have a significant effect on the levels in ^{59}Fe.

The results of McLean *et al.*[7] produced certain discrepancies with Sood's results. In particular, Sood fails to account for the two $\frac{3}{2}^-$ levels at 571 and 726 keV. McLean *et al.*[7] suggested that a different set of Nilsson-model parameters might better describe the ^{59}Fe nucleus without invoking bandmixing. The results of such a calculation using the method of Nilsson[18] are compared with

TABLE IV. Comparison with predictions of the mass excess and Q_β for ^{59}Mn.

Source	Mass excess (MeV)	Q_β (MeV)
This work	-55.5 ± 0.1	5.2 ± 0.1
Kashy *et al.* [a]	-55.49 ± 0.03	
MSMME [b]	-55.35	(5.31)
Myers [c]	-55.23	4.80 (5.43)
GHT [d]	-56.40	4.16 (4.26)
SH [e]	-55.6	4.4 (5.1)
LZ [f]	-56.08	4.33 (4.58)
BLM [g]	-53.5	4.3 (7.2)
JGK [h]	-55.94	4.61 (4.72)
Comay and Kelson [i]	-56.12	4.52 (4.54)
WBG [j]	-55.67	(5.00)

[a] E. Kashy *et al.*, Ref. 10.
[b] C. N. Davids, Ref. 19. Mass of ^{59}Fe not cited.
[c] W. D. Myers, Ref. 16.
[d] H. V. Groote, E. R. Hilf, and K. Takahashi, Ref. 16.
[e] P. A. Seeger and W. H. Howard, Ref. 16.
[f] S. Liran and N. Zeldes, Ref. 16.
[g] M. Beiner, R. J. Lombard, and D. Mas, Ref. 16.
[h] J. Jänecke, Ref. 16.
[i] E. Comay and I. Kelson, Ref. 16.
[j] A. H. Wapstra, K. Bos, and N. B. Gove, Ref. 20.

experiment in Fig. 7.

Comparing Fig. 7 with Fig. 3, one sees that only the 473-keV transition is an intraband transition. All other transitions are deexcitations by interband transitions in this model. Since $E2$ rates should be enhanced in intraband transitions, one would expect the second member ($J^\pi = \frac{3}{2}^-$) of the $K = \frac{1}{2}^-$ rotational band to have a transition to the $K = \frac{1}{2}^-$ bandhead. The 726-keV level is observed to have a transition to the 287-keV level, while no transition to this state is observed from the 571-keV state. This would suggest that the 726-keV level is the $\frac{3}{2}^-$ member of the $K = \frac{1}{2}^-$ rotational band. These considerations do not agree with those of McLean *et al.*[7] who based their assignment of the 571-keV level to the $K = \frac{1}{2}^-$ rotational band on the relation between observed and predicted spectroscopic factors. It may well be that a certain amount of bandmixing has occurred in these levels to account for the transitions observed.

C. Mass of ^{59}Mn

The values obtained for the ^{59}Mn mass excess from this work and that of Kashy *et al.*[10] are compared with various mass predictions in Table IV. The measured Q_β is also compared with the values predicted with a given model. The Q_β values not enclosed in parentheses use the mass excess of ^{59}Fe from the compilation of Wapstra and Bos.[16] The Q_β values in parentheses use the ^{59}Fe mass excess internally predicted.

The comparisons in Table IV show a rather wide scatter in the predicted values for the mass excess of ^{59}Mn. The modified shell-model mass equation (MSMME) results of Davids,[19] the droplet model of Myers,[16] and the droplet model plus shell correction prediction of Seeger and Howard[16] show the best agreement in the mass excess values.

Note added in proof: Recent in-beam γ-ray results of E. K. Warburton *et al.* (private communication) tend to favor a spin assignment of $\frac{5}{2}^-$ for the 571-keV state in ^{59}Fe. This assignment does not affect any conclusions in the present work.

ACKNOWLEDGMENTS

The authors would like to thank G. E. Thomas for producing the enriched ^{48}Ca foil targets used. Informative discussions with D. Kurath and S. L. Tabor are gratefully acknowledged.

*Present address: Cyclotron Laboratory, Department of Physics, Michigan State University, East Lansing, Michigan 48824.

†Work performed under the auspices of the USERDA, Division of Physical Research.

‡Alfred P. Sloan Foundation Fellow.

§Thesis student at Argonne from the University of Chicago.

‖Present address: Department of Physics, The Florida State University, Tallahassee, Florida 32306.

[1] C. N. Davids, E. B. Norman, R. C. Pardo, and L. A. Parks, Bull. Am. Phys. Soc. 20, 1164 (1975); in Proceedings of the Third International Conference on Nuclei Far From Stability, Cargèse, Corsica, 1976 (unpublished), CERN 76-13, p. 590.

[2] C. N. Davids, S. L. Tabor, E. B. Norman, R. C. Pardo, and L. A. Parks, Phys. Rev. C 14, 160 (1976).

[3] L. A. Parks, C. N. Davids, and R. C. Pardo, Phys. Rev. C 15, 730 (1977).

[4] A. Sperduto and W. W. Buechner, Phys. Rev. 134, B142 (1964).

[5] L. L. Lee, Jr., and J. P. Schiffer, Phys. Rev. 154, 1097 (1967).

[6] E. D. Klema, L. L. Lee, Jr., and J. P. Schiffer, Phys. Rev. 161, 1134 (1967).

[7] K. C. McLean, S. M. Dagliesh, S. S. Ipson, and G. Brown, Nucl. Phys. A191, 417 (1972).

[8] P. C. Sood, Phys. Rev. 179, 1100 (1969).

[9] P. C. Sood and D. A. Hutchinson, Nucl. Phys. A96, 159 (1967).

[10] E. Kashy, W. Benenson, D. Mueller, H. Nann, and L. Robinson, Bull. Am. Phys. Soc. 20, 1164 (1975); Phys. Rev. C 14, 1773 (1976).

[11] L. A. Parks, C. N. Davids, B. G. Nardi, and J. N. Worthington, Bull. Am. Phys. Soc. 21, 633 (1976); Nucl. Instrum. Methods (to be published).

[12] A. P. Bogdanov, V. A. Knat'Ko, A. V. Soroka, and V. N. Tadéush, Yad. Fiz. 14, 909 (1971) [Sov. J. Nucl.

Phys. 14, 509 (1972)].
[13]H. J. Kim, At. Data Nucl. Data Tables 17, 485 (1976).
[14]N. B. Gove and M. J. Martin, Nucl. Data Tables 10, 205 (1971).
[15]C. N. Davids, D. R. Goosman, D. E. Alburger, A. Gallman, G. Guillaume, D. H. Wilkinson, and W. A. Lanford, Phys. Rev. C 9, 216 (1974).
[16]S. Maripuu, Ed., At. Data Nucl. Data Tables 17, 477 (1976), 1975 Mass Excess Predictions.
[17]S. Raman and N. B. Gove, Phys. Rev. C 1, 1995 (1973).
[18]S. G. Nilsson, K. Dan. Vidensk. Selsk. Mat.-Fys. Medd. 29, No. 16 (1955).
[19]C. N. Davids, Phys. Rev. C 13, 887 (1976).
[20]A. H. Wapstra, K. Bos, and N. B. Gove, 1974 Supplement to the Atomic Mass Adjustment (private communication).